

A NANOSECOND BEAM PULSING AND TIME-OF-FLIGHT
SYSTEM FOR AN MP TANDEM

K. H. Purser, A. Bahnsen, and M. S. Krick
University of Rochester
Rochester, New York

Introduction

As the use of pulsed beams for producing nuclear interactions provides the instant of time at which the reaction took place, additional experimental information can often be extracted compared to experiments with d.c. beams. Specifically, with appropriate instrumentation, it is possible to measure the characteristic times of the reaction and the velocity of the reaction products. The most extensive use of these techniques has been for the direct measurement of neutron velocity spectra; today it is generally accepted that the combination of a pulsed accelerator and time-of-flight measurements represents the most reliable way of obtaining with precision neutron spectra in the 1-20 MeV range.

Although the major application in nuclear physics of pulsed beams has been, in the field of neutron spectroscopy^{1,2,3}, there are a variety of other uses. For example, timing can be used in the study of neutron-induced reactions to select primary neutrons having a specific energy from a broad distribution.⁴ It is also possible to make mass identification of the charged particles using a single solid-state detector, rather than the conventional E and dE/dx method.⁵ Timing can also be applied to reduce backgrounds which originate in the detector from radiations which arrive at a time which is known to be different from the arrival time of the wanted events. For example, in resonance fluorescence measurements at high proton energies, the background induced in the detector from fast neutron interactions are often prohibitively great. These backgrounds can be almost completely eliminated in a pulsed experiment as the neutrons arrive at the detector at a much later time than do the gamma rays from the target.⁶

General Description

A pulsed beam and time-of-flight system has been designed and is being installed on the MP tandem Van de Graaff at the University of Rochester's new Nuclear Structure Research Laboratory. The over-all arrangement of the pulsing system and the associated electronics is shown in Figure 1. A d.c. beam from the ion source, within the injector, is

chopped to provide 20-50 ns bursts at intervals of 400 ns, or some sub-multiple, and is velocity modulated by a buncher at ground potential to provide bursts of current at the target. The bursts of ions leaving the tandem will be chopped again by a high-energy sweeping system. The important function of this component is to remove particles that are not in the main burst and provide insurance against a loss of phase when the machine suffers a minor voltage surge. Preliminary measurements have shown that peak intensities of ~ 1 mA can be obtained with a pulse width ≤ 2 ns. With minor changes, it is expected that this burst width can be reduced to ~ 0.6 ns.

As the arrangement of the system is closely modeled upon the suggestions of Naylor, Purser, and Rose,⁷ the present paper does not discuss many of the fundamental considerations but only touches on the more important parameters and concentrates more on a description of the equipment that is presently being installed at Rochester.

Injector Chopping

Figure 2 is a schematic diagram showing the major components of the MP tandem's d.c. beam transport system.⁷ A variety of sources can be used within the injector for the production of negative ions with an energy that is variable but is typically in the range 40-80 keV. The negative ion beam from the source is focused, momentum analyzed to remove unwanted components, and injected into a short acceleration region where the ions are given additional energy before injection into the tandem. During pulsed operation, the aperture at the entrance to the pre-acceleration tube serves also to provide an opening across which the d.c. beam from the source can be deflected to produce beam bursts having an adjustable time-width in the range 20-50 ns. This chopping is essential to remove the particles which would arrive with the wrong phase at the buncher and thus would provide a dark current between beam bursts.

The arrangement of the chopping plates is shown in Figure 3. A 2.5 MHz sine wave is applied to one pair of plates. A second pair of plates, perpen-

dicular to the first, is connected to a 1 kV pulse generator which allows the beam to be unblanked every n -th cycle, where n is 1, 2, 4, 8, 16, 32. This arrangement allows the pulse-to-pulse time to be as short as 400 nS or as long as 12 μ S.

Bunching

After passing through the pre-acceleration potential (100-300 kV), the ions are focused by an electrostatic quadrupole triplet to an injection point on the tandem axis. This injection point is conjugate to the stripping canal with the optical focusing which couples these points being accomplished by the combined effects of the low-energy acceleration tubes and a gridded bipotential lens immediately preceding the first acceleration tube. During pulsed operations, a velocity modulator, located as close as possible to the injection point, is used to bunch the beam. There are important advantages in locating the buncher at this cross-over. In the first place, the ion energy at this point can be sufficiently high so that the energy inhomogeneities in the beam leaving the source contribute negligibly to the time spread of the final pulse. Secondly, because there are inevitably radial components in the electric field across the gaps in the modulator which cause the modulator to become a time-varying electrostatic lens, angular confusion is introduced into the beam. However, if the modulator can be located close to a cross-over, the introduced angular confusion has no effect on the diameter of the beam at this point and to first order has no effect on the diameter at the stripping canal. Measurements at Rochester have verified this prediction: A 5 MHz, 12 kV peak-to-peak signal on the central element of a two-gap buncher having 0.48 meters between the gaps shows the transmission through the accelerator to be reduced less than 5%. Finally, since the ion energy can be varied at the buncher, a wide variety of masses can be compressed without mechanical changes.⁷

Two effects limit the bunching ratios that can be obtained. The first of these limitations arises because the tandem optics are dispersive in energy, and there is a limit to the energy inhomogeneity that can be tolerated in the beam; energy inhomogeneities greater than this limit will put the particles so badly out of focus that they cannot reach the target. A second limitation arises because practical design considerations limit the bunching waveform to that of a sine wave;

such a waveform is far from the ideal (see equation 1) and automatically implies a major sacrifice of duty cycle and beam intensity.

Naylor et al⁷ have calculated the acceptable values of $\Delta E/E_0$ which can be imposed upon the beam if the diameter at the stripper is not to grow by more than 0.25 cm. The results of these calculations are listed in Table I with the final column showing the time-length of beam that can be compressed.

Table I
Acceptable Values of $\Delta E/E_0$

Terminal Voltage (MV)	$\Delta E/E_0$ (%)	Introduced ΔE $E_0=125$ keV (keV)	ΔE (nS)
1	4.8	12.0	30.5
3	6.1	15.2	38.5
5	6.9	17.2	44.0
8	7.3	18.2	46.0
10	7.8	19.5	49.4
12	8.1	20.5	52.0

Clearly, the use of foil stripping, which imposes less restrictions on the diameter of the beam at the terminal, will increase the acceptable values of $\Delta E/E_0$.

An analysis of the voltage waveform of a single-gap buncher shows that it should have the form

$$V(t) = K[t/t_0 + 3/2(t/t_0)^2 + 4/2(t/t_0)^3 + \dots] \quad (1)$$

$$= K' \frac{t}{t_c} [1 + \epsilon]$$

where $\epsilon = 3/2 (t/t_0) + 4/2(t/t_0)^2 + \dots$

t_0 = bunching time with no acceleration

K = constant of the ion beam and geometry

Now the difference between the sine wave and the ideal waveform is given by

$$\Delta V(t) = Kt[(1 + \epsilon) - (1 + \epsilon')] = Kt[\epsilon - \epsilon']$$

where $\epsilon' = \frac{\sin \omega t - \omega t}{\omega t}$

Figure 4 shows a plot of ϵt and $\epsilon' t$ as a function of t for the case of 125 keV protons, a bunching length of 3.25 meters, and a driving frequency of 5 MHz.

Also shown is the error curve for 5% greater amplitude than that given above and a leading phase for the injected burst of 10° .

From the error curves of Figure 4, it can be seen that it is possible to bunch up to a 50 nS length of beam. This means that the d.c. current for a repetition rate of 2.5 MHz is

$$|I| = \frac{50}{200} \times I_{d.c.}$$

Now, for protons and deuterons, $I_{d.c.}$ of 20 μ A is quite achievable so that $|I| \sim 3 \mu$ A and $I_{peak} \sim 1$ mA.

Measurements made recently at Rochester indicate that peak burst intensities of 0.5 mA were obtained by bunching a d.c. beam of 10 μ A. This is in excellent agreement with the above calculations.

Post-Acceleration Sweeping

It is planned that the bursts of ions leaving the tandem will be further chopped by a sweeping system located between the exit quadrupole and the object slits of the 90° analysis magnet. This system serves to remove particles which are not in the main burst and eliminates pulses whose phase is incorrect because of minor surges within the generator. Time dependent phase variations will be corrected by a circuit similar to that reported by Adelberger.⁸ It is anticipated that this chopping system will be used for two other special applications: First, in conjunction with neutral He^3 injection and bunching, it will provide intense nanosecond bursts of He^3 ; and secondly, it will permit isotope selection by measuring flight times through the complete accelerator.

The post-acceleration deflector box is shown in Figure 5. The beam for the accelerator passes between two 1-meter long parallel plates separated by 3 cm and is deflected vertically by a 10 MHz alternating field for chopping at vertical slits at the object point of the 90° analyzer. The major design requirements of this component were:

1. A maximum voltage of 50 kV peak at 10 MHz.
2. The field between the plates to be uniform over the cross section of the beam.
3. Low power consumption (10 kW max).

In order to avoid the problems and heating associated with vacuum feed-

throughs for r.f., the resonant inductance is mounted inside the vacuum enclosure with the deflector plates. Quartz is used exclusively for support and insulation due to its low loss factor, its mechanical rigidity, and its low coefficient of expansion.

Figure 6 shows a cross section of the deflector plates and the electrostatic field between them. It can be seen that the field is quite uniform over a diameter of 2.5-3.0 cm as a consequence of the bulges that are built into the edges of the plates. The advantage of this design over flat plates is that they can be narrow with a minimum of capacity and a minimum of circulating current in the tank circuit.

The coil was designed to achieve a high Q by using a minimum of low-loss dielectrics and using silver-plated heavy conductors on a large winding diameter. A preliminary measurement on this coil indicates a Q of about 500. Although this is quite high, it still means that about 2.5 kW will be dissipated in the coil, which is water-cooled.

The power necessary to overcome these losses is supplied from a 10 kW amplifier whose circuit is shown in Figure 7. This power is delivered to the sweeping box through a 125 ohm coaxial line, which is matched to the tank coil of the resonant circuit by using the resonant inductance as the secondary of a transformer, the primary being formed by a grounded loop of the central conductor of the coaxial line.

Post-Acceleration Beam Transport

Somewhat surprisingly, the largest contribution to time spread in the beam burst at the target arises in the MP tandem from differences in path lengths within the beam transport system. The most serious dispersion arises within the deflecting magnets as median plane focusing is obtained by causing the outer trajectories to travel a greater distance within the magnetic field and to be deflected through greater angles. It can be easily shown that, for realistic emittances, these effects introduce several nanoseconds time spread for the hydrogen isotopes.⁷

Although beams of finite emittance passing through a simple magnet show an increase in pulse length, the time information within the beam is not irretrievably lost as space-time correlations still exist. Thus, if the particle

trajectories are passed through a second bending field, which is mirror symmetrical to the first, about a plane normal to the beam located at a cross-over point, the debunching effects can be eliminated. The design of such isochronous and non-dispersive deflection systems have been considered by a number of authors (see ref. 9). Figure 8 shows the principles of the post-acceleration system that is being installed at Rochester for isochronous transport of the beam between the tandem and the target location. An important change to the conventional optics is that considerably more space is available between the analyzing magnet and the switching magnet, so that an extra quadrupole focusing element can be introduced at the image slits of the 90° analyzer to produce the focal points that are planned at the symmetry planes of the deflecting magnets.

In order to evaluate various possible arrangements of components, a linear ray tracing program was written to carry out successive matrix multiplications for the various elements in the system. The isochronous properties were evaluated by extending the matrix formulation described by Penner^{7,10} to a 6x6 vector space, where the additional parameter to the radii, angles, and momentum spread is the incremental length between particular trajectories and the axial ray. The trajectory calculations that were made showed that, in the revised system, although time spreads are still present and are proportional to the emittance of the beam, they are of magnitude 0.05 nS for our geometry. This time is sufficiently short so that the limitation of the over-all pulsing system becomes the waveform inaccuracies in the shape of the bunching waveform.

270° Rotating Magnet

If neutron studies are to be really useful, a high resolution neutron spectrometer is essential. When realistic resolving times of the detectors and electronics are included as design parameters (~ 1.5 nS), it becomes clear that the flight paths must be long (20-40 meters) to obtain good resolution for neutrons with energies above a few MeV.

Among tandem facilities, Rochester is somewhat unique in that the facility has in one direction a flight path of up to 60 meters. This flight path passes through the shielding wall (see Figure 9), allowing the detectors to be used in an annex outside of the main target area. At first sight, such an arrangement seems

to preclude the measurement of angular distributions. However, this is not so as it is only necessary to change the angle between the incident beam and the flight path; and it is planned that the incident beam be rotated about the target keeping the detector fixed rather than the conventional system of multiple detectors and flight paths.

The arrangement of magnets to be used for this rotation of the incident beam is shown in Figure 10 and is based upon a suggestion of H. Enge.¹¹ The two magnets are arranged so that beam is deflected first in the horizontal plane into a direction which is at right angles to the axis of the time-of-flight tunnel. The beam then enters the 270° magnet which is mounted to allow rotation about the direction of the incident beam. In this way, it is possible to measure 0-360° angular distributions with a large single detector in a fixed location.

Bibliography

1. Havens, W. W., Jr., Proc. Int. Conf. on Peaceful Uses of Atomic Energy 4, 74 (1956)
2. Parker, V. E., and King, R. F., Bull. Am. Phys. Soc. 1, 70 (1956)
3. Neiler, N. H., and Good, W. M., Fast Neutron Physics I (Interscience, 1960)
4. Barschall, H. H., Nuclear Instr. and Methods 28, 44 (1964)
5. Gemmel, D. S., Ninth Scintillation and Semiconductor Conference (Feb., 1964)
6. Skorka, S. J., Nuclear Instr. and Methods 28, 192 (1964)
7. Naylor, H., Purser, K. H., Rose, P. H., IEEE Transactions on Nuclear Science, June, 1965
8. Adelberger, E. (Private Communication) Submitted to Nuclear Instr. and Methods
9. Steffen, K. G., High Energy Beam Optics (Interscience, 1965)
10. Penner, S., R.S.I. 32, 150 (1961)
11. Enge, H. A. (Private Communication)

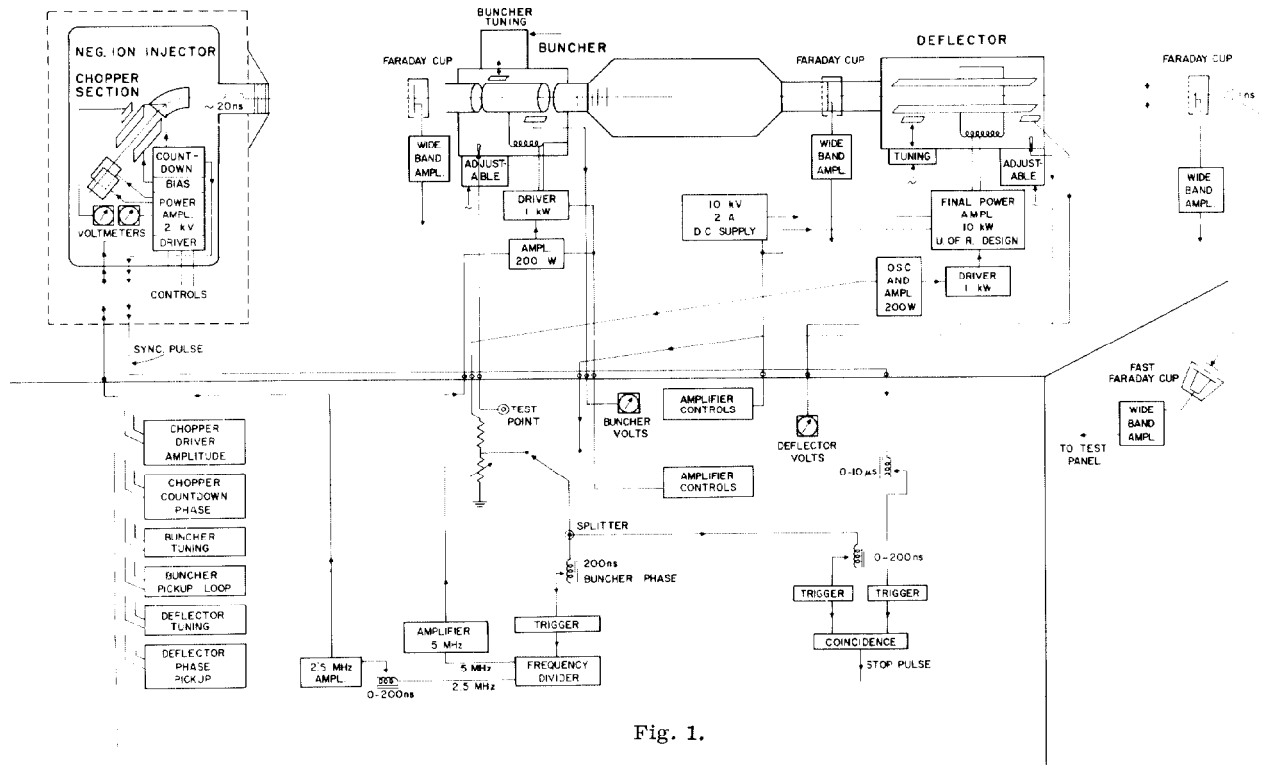


Fig. 1.

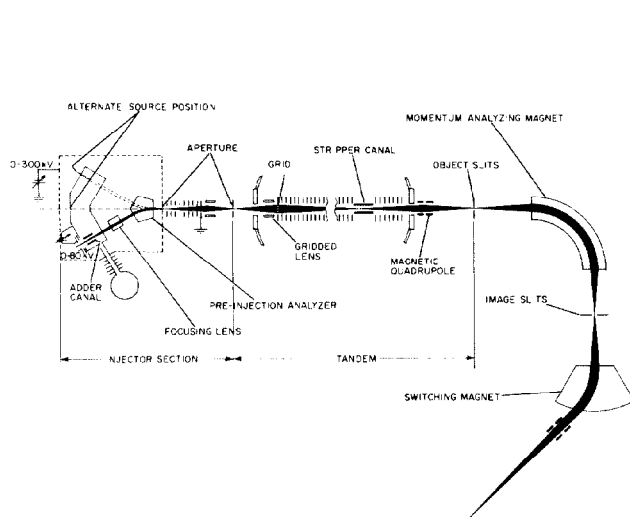


Fig. 2.

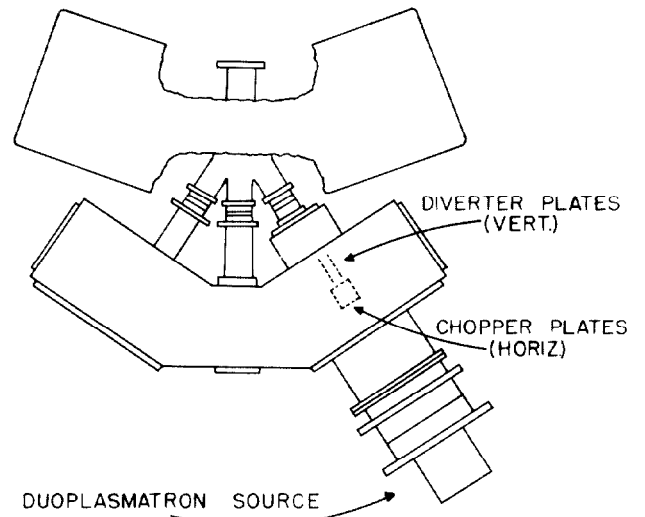


Fig. 3.

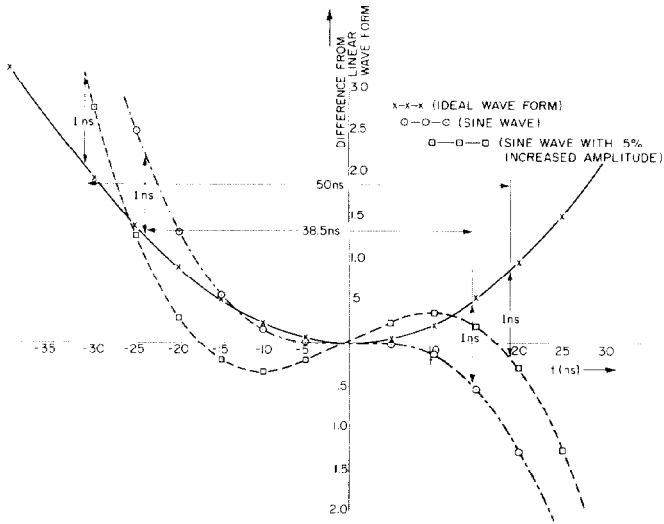


Fig. 4.

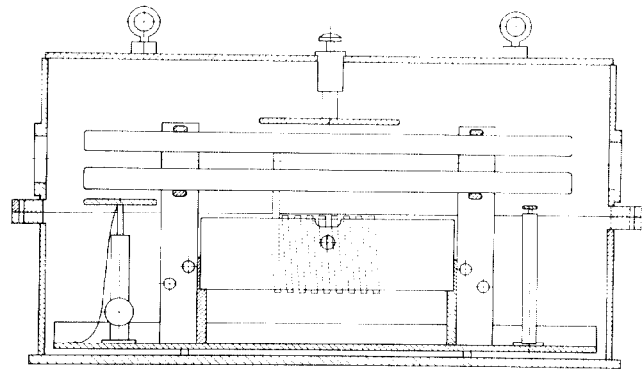


Fig. 5a.

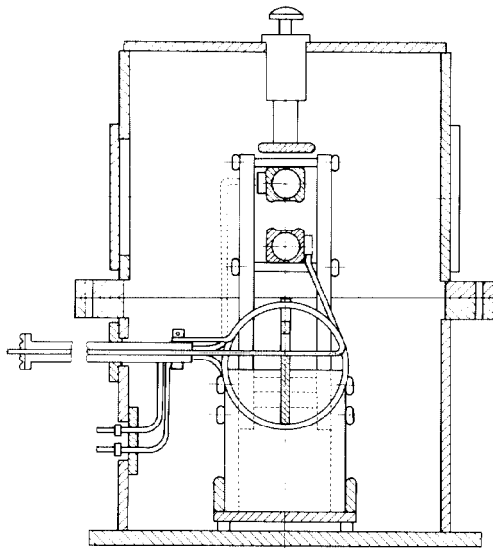


Fig. 5b.

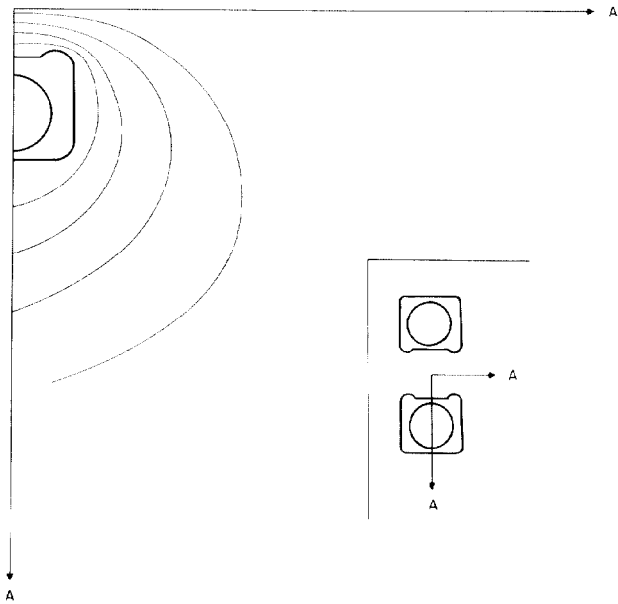


Fig. 6.

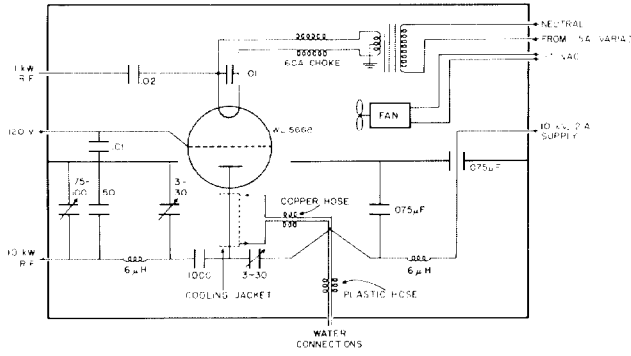


Fig. 7.

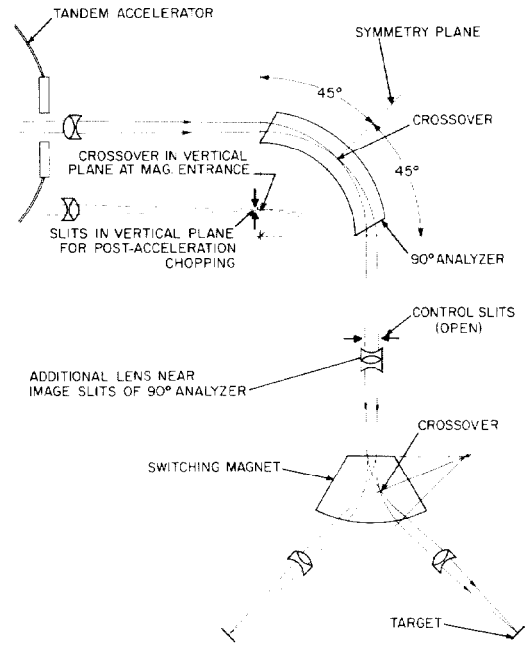


Fig. 8.

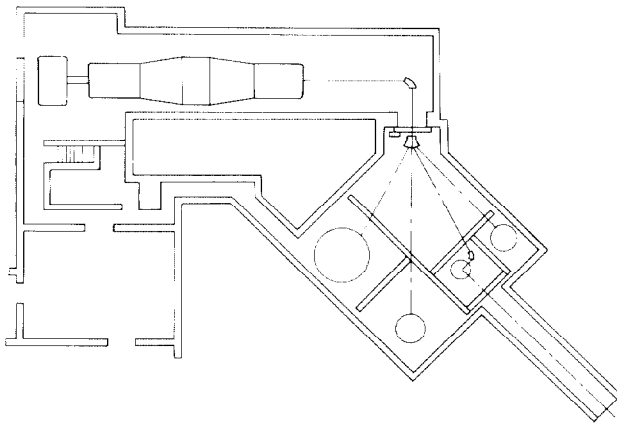


Fig. 9.

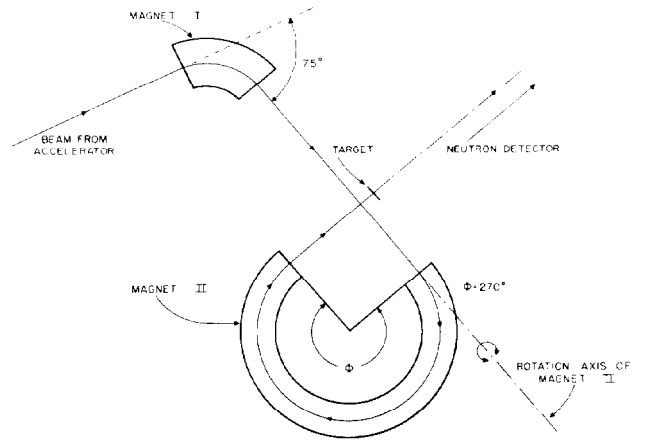


Fig. 10.